A regional (land–ocean) comparison of the seasonal to decadal variability of the Northern Hemisphere jet stream 1871–2011

Samantha Hallam[1,2,3] · Simon A. Josey[2] · Gerard D. McCarthy[1] · Joël J.-M. Hirschi[2]

Abstract

Seasonal to decadal variations in Northern Hemisphere jet stream latitude and speed over land (Eurasia, North America) and oceanic (North Atlantic, North Pacific) regions are presented for the period 1871–2011 from the Twentieth Century Reanalysis dataset. Significant regional differences are seen on seasonal to decadal timescales. Seasonally, the jet latitude range is lower over the oceans compared to land, reduced from 20° over Eurasia to 10° over the North Atlantic where the ocean meridional heat transport is greatest. The mean jet latitude range is at a minimum in winter (DJF), particularly along the western boundary of the North Pacific and North Atlantic, where the land-sea contrast and SST gradients are strongest. The 141-year trends in jet latitude and speed show differences on a regional basis. The North Atlantic has significant increasing jet latitude trends in all seasons, up to 3° in winter. Eurasia has significant increasing trends in winter and summer, however, no increase is seen across the North Pacific or North America. Jet speed shows significant increases evident in winter (up to 4.7 ms^{-1}), spring and autumn over the North Atlantic, Eurasia and North America however, over the North Pacific no increase is observed. Long term trends are generally overlaid by multidecadal variability, particularly evident in the North Pacific, where 20-year variability in jet latitude and jet speed are seen, associated with the Pacific Decadal Oscillation which explains 50% of the winter variance in jet latitude since 1940. The results highlight that northern hemisphere jet variability and trends differ on a regional basis (North Atlantic, North Pacific, Eurasia and North America) on seasonal to decadal timescales, suggesting that different mechanisms are influencing the jet latitude and speed. This is important from a climate modelling perspective and for climate predictions in the near and longer term.

Keywords Northern Hemisphere jet stream · Ocean–Atmosphere Interactions · Decadal trends · Jet stream variability · Twentieth Century Reanalysis

1 Introduction

Jet streams are fast, narrow air bands, which flow around the globe in both hemispheres at around 10,000 m (Archer and Caldeira 2008). The flow is predominantly zonal from west to east with jet speeds reaching 45–70 ms^{-1} and possibly higher in winter (Barry and Chorley 2009). Each hemisphere has a polar front jet (PFJ) and a subtropical jet (STJ). The PFJ, also referred to as the eddy-driven jet (EDJ), forms along the polar front in the region where there is a sharp temperature contrast which drives the formation of the baroclinic eddies (Pena-Ortiz et al. 2013; Holton 1992). The STJ is driven by 2 mechanisms and forms on the poleward side of the Hadley cell (Pena-Ortiz et al. 2013). The STJ is mainly a consequence of the conservation of angular momentum which means that air masses flowing poleward in the upper Hadley cell experience a westward deflection (Lee and Kim 2003).

Jet stream variations have a significant impact on storm activity and temperature patterns across the northern hemisphere, and accordingly impact the environment and society. Jet streams and their seasonal to decadal variability form an important part of natural climate variability due to their influence on the mid latitude storm tracks (Hurrell 1995), which form in the region ahead of an upper level

✉ Samantha Hallam
  samantha.hallam@mu.ie

1   Irish Climate Analysis Research Units, Maynooth University, Maynooth, Ireland

2   National Oceanography Centre, European Way, Southampton SO14 3ZH, UK

3   University of Southampton, National Oceanography Centre, European Way, Southampton SO14 3ZH, UK

trough where reduced cyclonic vorticity causes divergence, favouring surface convergence, cyclonic circulation and storm track formation (Barry and Chorley 2009). In winter storm tracks bring heat and moisture to regions that would otherwise be cooler and drier. They can also cause extreme weather events, both of which have a significant impact on society (Trenberth and Hurrell 1994). Jet stream variability is therefore an important component of climate 'noise' and understanding the seasonal to decadal variability can help inform the study of what climate change will look like on a regional basis e.g. Ronalds et al. (2018) and Barnes and Simpson (2017).

Long term jet stream changes are potential indicators of a changing climate (Pena-Ortiz et al. 2013) and several studies have found evidence for a poleward shift in the jet streams and storm tracks (Hartmann et al. 2013). Archer and Caldeira (2008) found a poleward migration in the Northern Hemisphere Jet (NHJ) of 0.17–0.19° per decade using NCEP-NCAR reanalysis data from 1958 to 2007, defining the NHJ as a single band spiral like structure "beginning south of the canary Islands and ending one eastward circumnavigation later over England". Pena-Ortiz et al. (2013) found the winter NHJ had moved poleward by 0.02° to 0.13°/decade using NCEP/NCAR (1979–2008) and the Twentieth Century Reanalysis (1958–2008) datasets. Fu and Lin (2011) suggest the STJ has shifted poleward by $1° \pm 0.3°$ between 1979 to 2009. Woollings et al. (2014) found a poleward shift of the EDJ (0–60° W) of 0.2°/ decade using the Twentieth Century Reanalysis dataset covering the period from 1871–2008. In terms of jet speed, Strong and Davis (2007) found increases up to 15% in the EDJ mean speed between 1958 and 2007, whilst Archer and Caldeira (2008) found a decrease of -0.2 ms^{-1}/decade in the NHJ. Whilst the studies are not directly comparable, as they cover different time periods, jet definitions, dataset used and geographical area studied, they do all suggest a poleward shift in the northern hemisphere jet stream. Most of the above studies are of the recent past (1958 onwards) and only Woollings et al. (2014) looked at data from 1871 but only for the North Atlantic. The first key motivation for the work here is to study the whole northern hemisphere, for the longest available time period from 1871, using one methodology and dataset.

The second motivation is to undertake a regional comparison to identify differences in northern hemisphere jet variability between land and ocean areas as recent research suggests land–ocean temperature contrast, ocean fronts and SST gradients can influence the storm track. For example, the studies by (Sheldon and Czaja 2014) and (Czaja and Blunt 2011) suggest western boundary ocean currents (WBC), through deep atmospheric convection, can influence the entire troposphere on interannual and decadal time-scales. Minobe et al. (2008) found that strong SST gradients led to atmospheric pressure adjustments which resulted in surface wind convergence, and effectively anchored the storm track. Strong sea surface temperature (SST) gradients found along ocean fronts and where cold air from continents flows over warm waters provide an environment for differential sensible and latent heating, which enhances baroclinicity (Hoskins and Valdes 1989), and leads to surface cyclonic wind convergence and effectively 'anchors' the storm track (Nakamura et al. 2004; Minobe et al. 2008). Small et al. (2014) also found that the storm track response to ocean fronts extended into the deep troposphere.

In other studies O'Reilly and Czaja (2015) highlight that the changes in the jet stream and storm track over the western Pacific are linked to variations in the Kuroshio Extension Front. When the surface SST gradient was strong the storm track was zonally localised, but there was less influence on the storm track location when the SST gradient was weaker in the 19-year period analysed. In addition, Gan and Wu (2013) found in the North Pacific that cold SST anomalies, typically -0.6 °C, north of 30° in autumn led to an increase in baroclinicity and poleward intensification of the storm track in early winter.

In the North Atlantic, Feliks et al. (2011, 2016), have shown that strong SST gradients along mid latitude ocean fronts have a significant influence on the jet stream diffluence angle and low frequency variability. O'Reilly et al. (2016) identified that the Gulf Stream SST front was important in the development of the storm track over the North Atlantic and also influenced European blocking development. Gan and Wu (2014) found that SST anomalies in November and December can influence storm tracks in the following March.

In addition, Woollings et al. (2015) and Fang and Yang (2016) found that cold subpolar SST anomalies influence the atmosphere by strengthening the meridional temperature gradient and baroclinity leading to intensification of the westerly jet stream, in the Atlantic and North Pacific, respectively.

As oceanic influences on the jet stream are now increasingly considered to be important (Simpson et al. 2019) this study looks at seasonal to decadal northern hemisphere jet stream variability, and the differences over ocean basins compared to land masses in terms of patterns of variability and long term trends. The northern hemisphere jet stream is analysed over 4 regions; North Atlantic (60° W–0° W), Eurasia (0–120° E), North Pacific (120° E–120° W) and North America (120° W–60° W). Only the northern hemisphere is included in view of the more significant land mass to provide a comparison to the ocean basins and to manage the scope of the study. Pena-Ortiz et al. (2013), Manney and Hegglin (2018) and Spensberger and Spengler (2020) also highlighted that understanding jet stream trends on a regional basis was important.

A regional (land/ocean) jet stream analysis, using one methodology and a long dataset does not appear to have been accomplished yet and will provide a broader understanding of the natural variability, decadal trends and be comparable regionally. Ensuring the full regional range of natural jet variability is captured in climate models (Iqbal et al. 2018; Barnes and Simpson 2017), is important for regional climate predictions. Alongside this, the regional longer-term trends in jet latitude and speed will either confirm or challenge studies, which are based on shorter timescales.

2 Data

To understand the jet stream variability the Twentieth Century Reanalysis (V2) (20CR) is used, covering the period from 1871 to 2011. 20CR is based on an ensemble method, with 56 ensemble members. The 20CR fields used here are: air temperature, wind velocities and geopotential height.

20CR is a global atmospheric circulation reanalysis dataset, which assimilates only surface pressure observations and uses an ensemble Kalman Filter data assimilation method and one global numerical weather prediction model (Compo et al. 2006, 2011). Compo et al. (2006), Whitaker et al. (2004), and Anderson et al. (2005) have all shown that reliable reanalyses can be obtained of earlier periods, where only sparse data are available, using only surface pressure observations where standard corrections are known, when combined with more advanced data assimilation methods. Compo et al. (2006), highlighted that compared to other assimilation methods, using an ensemble Kalman filter provides results which not only cover large scale features, but also many synoptic features and had a smaller analysis error when observations are sparse. For the northern hemisphere extratropics (20° N–90° N) in the upper troposphere, the zonal and meridional wind components have an error and anomaly correlation skill at a level of 0.8 or above from 1895 onwards, for both summer and winter. Compo et al. (2006) find the analysis error to be equivalent to the modern NWP 2–3-day forecast error in the middle and upper troposphere. This forecast error is based on 1979–2001 reforecast skill using a 1998 NCEP model and NCEP-NCAR reanalysis. From this Compo et al. (2006) conclude that 20CR is suitable to reanalyse the entire extratropical tropospheric circulation which provides confidence in using 20CR for this study. The summer analysis errors are, however, larger than in winter, which was also identified by Ferguson and Villarini (2014).

Utilising only surface pressure reports to compile the dataset can help overcome issues from differing conventional observations (Pawson and Fiorino 1999). For example Archer and Caldeira (2008) used the ERA-40 and NCEP/NCAR datasets but only for the period from 1979 when satellite observations were available due to the differences seen in the dataset once satellite observations were introduced. To manage the scope of this study we only analyse the 20CR dataset and accept this may limit some of the uncertainty estimates on trends identified. 20CR has been compared to NCEP/NCAR, however, in other similar studies. Woollings et al. (2014) compared North Atlantic Jet latitude and speed from the NCEP-NCAR reanalysis and found "extremely good agreement" with jet latitude, for the period from 1948, with the 20CR data as outlined in their Fig. 7. For jet speed, outlined in their Fig. 8, they found good agreement although jet speeds were consistently slightly weaker in 20CR in all seasons. Pena-Ortiz et al. (2013) also analyse jet stream trends for the for the whole northern hemisphere for the period from 1958–2008 using both 20CR and NCEP/NCAR data and find similar results using both datasets. Both these studies help to confirm the suitability of 20CR for this study.

3 Methodology

Using appropriate indices to define the jet stream and validating the robustness of the 20CR data is an important part of the study and is discussed in this section.

Jet streams are diverse in nature and can vary spatially and temporally. The main approaches adopted to define the jet stream are either, the *maximum* wind speed over one or more isobaric levels, or the *average* wind speed over 30 ms^{-1} across one or more isobaric surfaces. Woollings et al. (2014) used the maximum zonal wind at the 850 mb level after establishing that the results were almost identical to averaging over 925–700 mb level. Pena-Ortiz et al. (2013) used the maximum zonal wind above 30 ms^{-1} and frequency at each longitude across the 400–100 mb level. Frequency of the jet over 30 ms^{-1} was also used by Kuang et al. (2014). Koch et al. (2006), and Strong and Davis (2007) used maximum wind speed above 30 ms^{-1} and 27 ms^{-1} respectively. Archer and Caldeira (2008) used the mass weighted monthly wind speed averages of the zonal and meridional components between 400 and 100 mb, whilst (Gan and Wu 2013) used the 300 mb meridional wind velocity to define the jet stream. However, in all of these studies whether a single isobaric level or a more complex approach was adopted (for example by Archer and Caldeira (2008)), only a single jet structure was identified. This suggests that either a single isobaric level or average over more isobaric levels is appropriate for defining the jet stream.

In this study a combination of the above approaches has been used. In line with Archer and Caldeira (2008), the absolute wind speed has been based on the zonal and meridional (u and v) wind velocity components, to ensure that meridional excursions in the jet stream paths are well captured.

As absolute wind speeds are being computed from the zonal and meridional components, it is important to ensure that the absolute wind speeds ($\overline{U}$) are calculated based on each of the ensemble members:

$$\overline{U} = \frac{1}{n}\sum_{i=1}^{n}\left(u_i^2 + v_i^2\right)^{0.5} \tag{1}$$

where, $u_i v_i$ are the zonal and meridional wind components and n = 56 is the number of ensemble members.

Accordingly, the wind components used to define the jet stream are the 6-hourly 250 mb meridional and zonal wind velocity, for each of the 56 20CR ensemble members, spanning the 141 year period from 1871 to 2011, at 2° longitude-latitude horizontal resolution (Compo et al. 2011). 250 mb is close to where the maximum velocity is observed (Fang and Yang 2016).

The maximum windspeed was used to define jet latitude and jet speed, in line with the methodology adopted by (Woollings et al. 2010, 2014). The algorithm used to calculate the jet stream proceeds as follows. First the 250mb 6-hourly zonal and meridional wind velocity for each of the 56 ensemble members for each year were obtained and the average absolute velocity $\overline{U}$ is calculated according to Eq. 1. The jet speed was defined as the maximum value of $\overline{U}$ at each longitude. The jet latitude was defined as the latitude of the maximum average absolute wind velocity ($\overline{U}$ maximum), for each longitude.

To provide a regional (land–ocean) comparison of the variability of the jet stream, the northern hemisphere was split into 4 regions (2 land and 2 ocean) which are shown in Fig. 1, Eurasia (0–120° E), North Pacific (120° E–120° W), North America (120° W–60° W), and North Atlantic (60° W–0° W). 60° W–0° W was used to define the North Atlantic to provide consistency with previous studies of the North Atlantic jet stream which also use this longitude range (Woollings et al. 2010, 2014). 120° E was used for the western boundary of the North Pacific region to ensure the Kuroshio current was included.

The regional approach, using one methodology and dataset, provides an opportunity to identify differences in regional variability and trends and help to identify if different mechanisms are influencing the jet stream across the four areas. It is accepted, however, that using a regional zonal mean may, however, mask variability and trends within that region.

The robustness of the dataset was assessed by considering the jet latitude and jet speed variance of the ensemble members (ensemble spread) over the 141-year time period and considering data inhomogeneity found in other atmospheric studies analysing 20CR. To understand the variance of the ensemble members, 3 separate jet latitude standard deviations were calculated; based on the 6-hourly data, based on the 6-hourly data smoothed over 31 days and based on the 6-hourly data smoothed over 91 days, using a Parzen filter. The timeseries results are illustrated in Fig. 2. A seasonal cycle is evident. The standard deviations reach maximum values in summer and minimum values in winter. The range reduces significantly over the period from 1871 to 2011. The largest variability is where no smoothing has been applied. There is a marked reduction in the jet latitude range during the 1930s to 2° and 1° when the standard deviations are smoothed by applying a low pass filter across the 56 ensemble members over 31 days and 91 days, respectively. Before the 1940s, the standard deviation range is higher across the ensemble members, in all regions, indicating a higher level of uncertainty. This is caused by lower data coverage to constrain the model in the early part of the record as highlighted by Wang et al. (2013) who show that standard deviation ensemble spread is directly related to the data points per 5 × 5 degree grid box. Their study shows that between the 1930s-1940s the number of data points increased from around 50 to 150 per grid box with a corresponding decrease in the ensemble spread.

Statistical data inhomogeneity may also play a role as outlined by Ferguson and Villarini (2014). They highlight that non-climate (unphysical) breaks in 20CR are at a maximum in July and detected what they suggest are several non-climate breaks in the northern hemisphere between the 1930s and 1940s. Incorporating data inhomogeneity into the interpretation of results was also highlighted by Woollings et al. (2014). Accordingly, throughout this study analysis is shown for periods 1871–2011 and 1940–2011, where appropriate. Comment is also made where trends vary between the 2 periods. For summer (JJA) only the period after 1940 is considered as the standard deviation of the ensemble members is greatest in that season and the data shows a pronounced step pre and post 1940s (Fig. 6).

Fig. 1 Regional view of the land and ocean areas considered overlaying the annual average 2 m air temperature. Eurasia (0—120° E), North Pacific (120° E–120° W), North America (120° W-60° W), and North Atlantic (60° W–0° W)
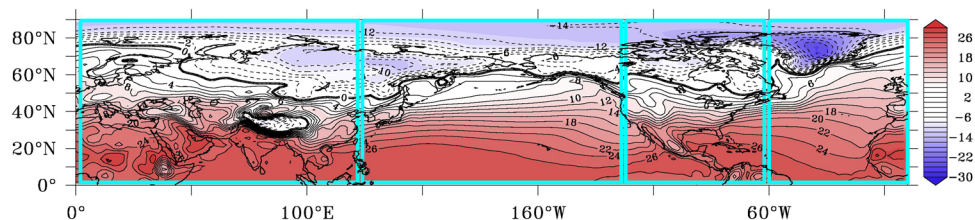
Fig. 2 Regional jet latitude standard deviations across the 56 ensemble members from 1871 to 2011. Blue line—Standard deviation based on the 6-hourly data across the 56 ensemble members. Green line—Standard deviation based on the 6-hourly data smoothed over 31 days by applying a low pass filter across the 56 ensemble members. Black line—Standard deviation based on the 6-hourly data smoothed over 91 days
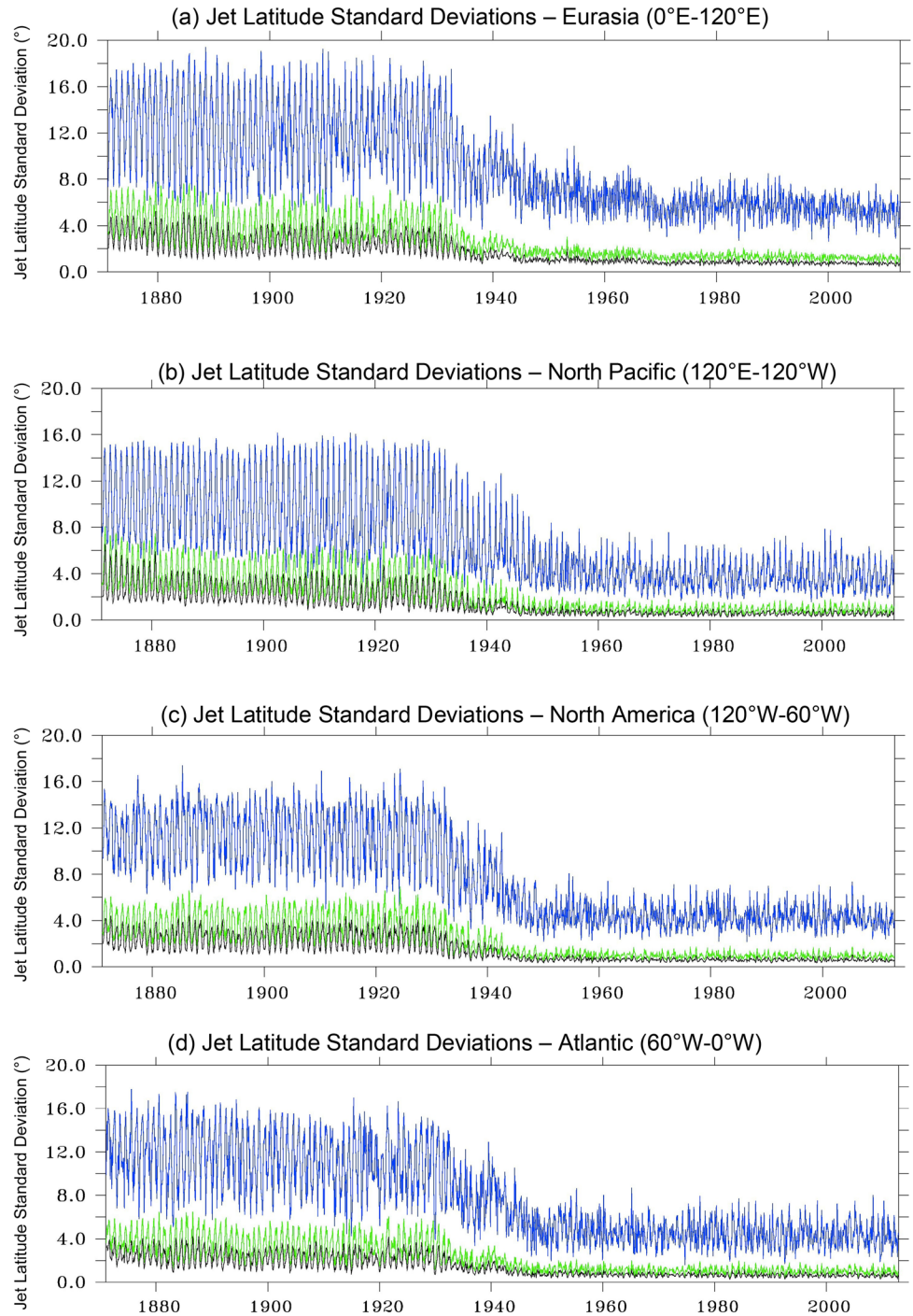
Separate jet speed standard deviations were also calculated on the same basis with similar results (not shown). Importantly, the ensemble spread, is broadly the same across all regions, for the corresponding time period when smoothed over 31 and 91 days, indicating that all regions can be used for this study.

To assist the analysis and understanding of the jet stream variability, this study also uses air temperature, and geopotential height data. For consistency, data from the 20CR dataset for the period 1871–2011 are used. Air temperature data is obtained from the 2 m air temperature monthly ensemble mean, and tropopause monthly ensemble mean. Geopotential height data is obtained from the 300mb geopotential height monthly ensemble mean.

4 Results

This section outlines the key findings from this study, first covering the seasonal variation in the jet latitude and speed, highlighting the variations over land masses compared to the ocean basins, before looking at the inter-annual variability and decadal trends. Where appropriate the results are shown for two periods 1871–2011 and 1940–2011. The latter period is used for comparison, as the spread across the ensemble members is significantly lower after 1940 (Fig. 2) as discussed.

4.1 Seasonal jet latitude and speed climatology

The jet latitude seasonal cycle (Fig. 3) shows a poleward shift in summer, but there are regional variations in the amplitude and lag with respect to insolation. For the full

Fig. 3 Seasonal Cycle of the Jet Stream Latitude in the Northern Hemisphere by region for periods 1871–2011 (**a**, **c**, **e**, **g**) and 1940–2011 (**b**, **d**, **f**, **h**). Black line is mean jet latitude. Grey area is ±2 standard deviations smoothed over 31 days using a Parzen filter based on the 56 ensemble members. Green line is ±2 standard deviations based on the interannual variability for the period
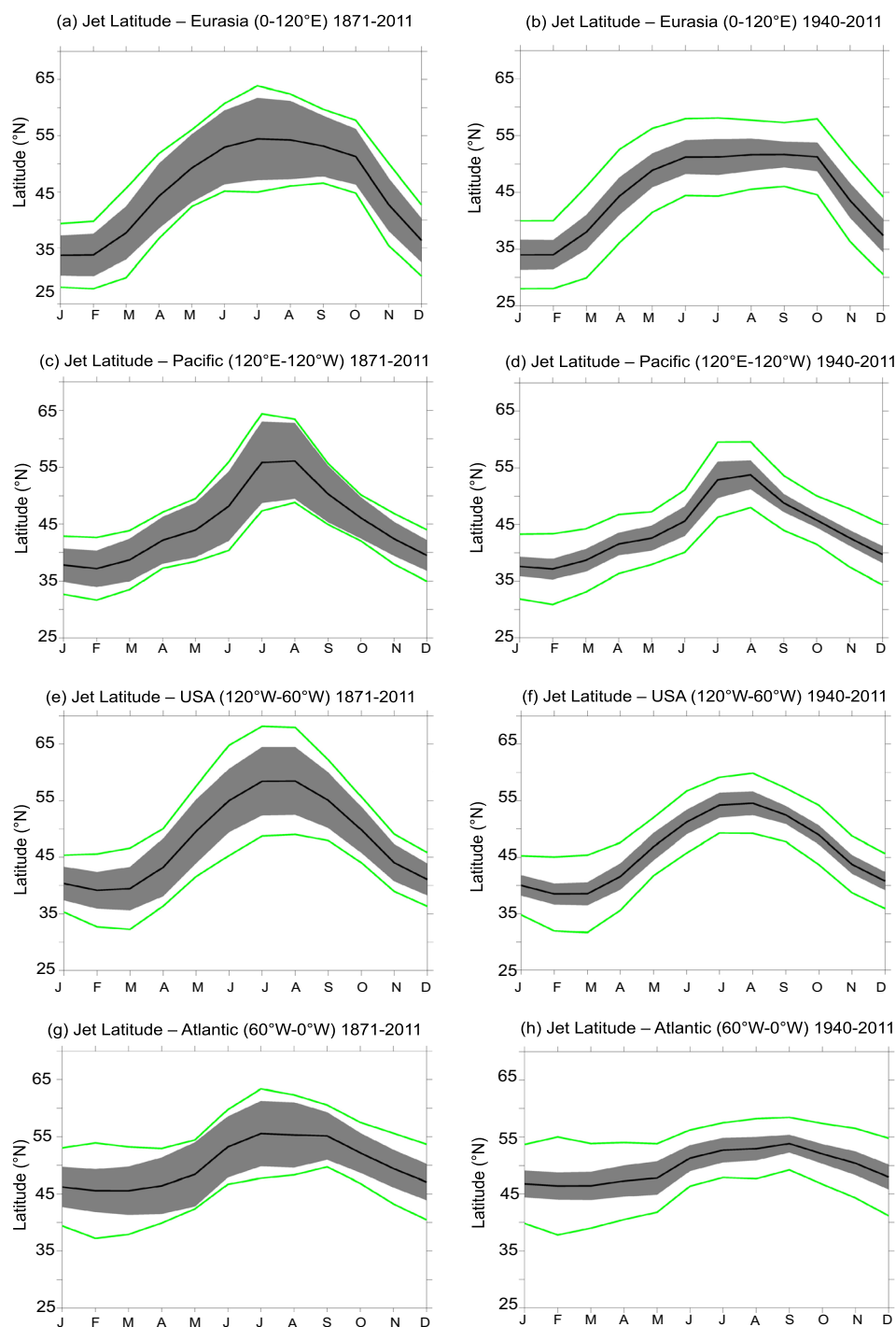
analysis period from 1871 to 2011 (Fig. 3a, c, e, g), the jet latitude amplitude is greatest over land; for Eurasia and North America the range is 20° from 34–54° N and 39–59° N, respectively. Over the North Atlantic the seasonal range is lower at 10° from 46–56° N and over the North Pacific the range is about 15° with a narrow peak in July and August. Only considering the 1940–2011 period (Fig. 3b, d, f, h) we find a reduction in the peak latitude in the summer months by around 3° over land and 2° over the ocean basins. Again, the jet latitude amplitude remains greatest over land; with a maximum for Eurasia of 18° whilst the North Atlantic range is only 7°. There is little difference for the interannual variability between the two periods whereas the uncertainty related to the ensemble spread is much reduced for the 1940–2011 period.

The seasonal cycle curves also have different shapes. In all regions there is a response of the jet stream to insolation. Over North America the response of the jet stream broadly follows a sinusoidal curve which lags insolation by about 1–2 months. The peak is broader over Eurasia, particularly for the period 1940–2011. Between February and June, the jet stream moves to its northernmost latitude at around 50° N, it then plateaus at this latitude until October, after which there is a steep decline. The North Atlantic shape is different again and a lag to insolation is evident. There is a broad flat line from January to May with only a 1° increase in latitude. From May onwards there is a 6° increase to September, before a steady fall from September to December. For the 1940–2011 period the seasonal cycle is barely significant and the interannual variability found for any given month largely overlaps with the interannual variability for any of the other months. Over the North Pacific the jet latitude slowly increases from February to June and a narrow peak is reached in July/August which is followed by a steady southward movement from October onwards.

The seasonal cycle of jet speed (Fig. 4) shows a similar pattern across land and the North Atlantic and displays a near-sinusoidal curve with maximum wind speeds seen in January around 59 ms^{-1} and minimum in July around 40 ms^{-1}. The cycle over the North Pacific resembles the inverse cycle seen for jet latitude, with a steep decrease in speed from May to July and steep increase from August to October. Speeds are also highest over the North Pacific, reaching a maximum in January at 66 ms^{-1} and minimum in July at 38 ms^{-1}. The average jet speed for each region and season is also over 35 ms^{-1} for each longitude (not shown). The main change observed between the 1871–2011 and 1940–2011 is that in the latter period the summer speeds have decreased by around 3 ms^{-1} to 39 ms^{-1}, whilst winter speeds have increased across North America and the North Atlantic.

Looking at the seasonal variations across the northern hemisphere (Fig. 5) indicates that the zonal variability in jet stream latitude is greatest in the winter months (DJF), resulting in a wave like pattern, with two latitude maxima located over the eastern Pacific and Atlantic. The jet stream follows a well-defined path in winter which is tightly confined, particularly on the western boundary of the North Pacific (33° N) near the Kuroshio current and North Atlantic (41° N) aligning with the Gulf Stream/North Atlantic Current. The jet stream troughs are also located in these areas in winter; the main areas for cyclogenesis. In spring (MAM) and autumn (SON) the jet stream troughs are further north, but remain over the western boundaries of the North Pacific (37° N, 41° N) and North Atlantic (43° N, 47° N) respectively. In summer (JJA) the jet stream follows a more zonal path around 55° N with the main ridge west of Hudson Bay (60° N, 100° W).
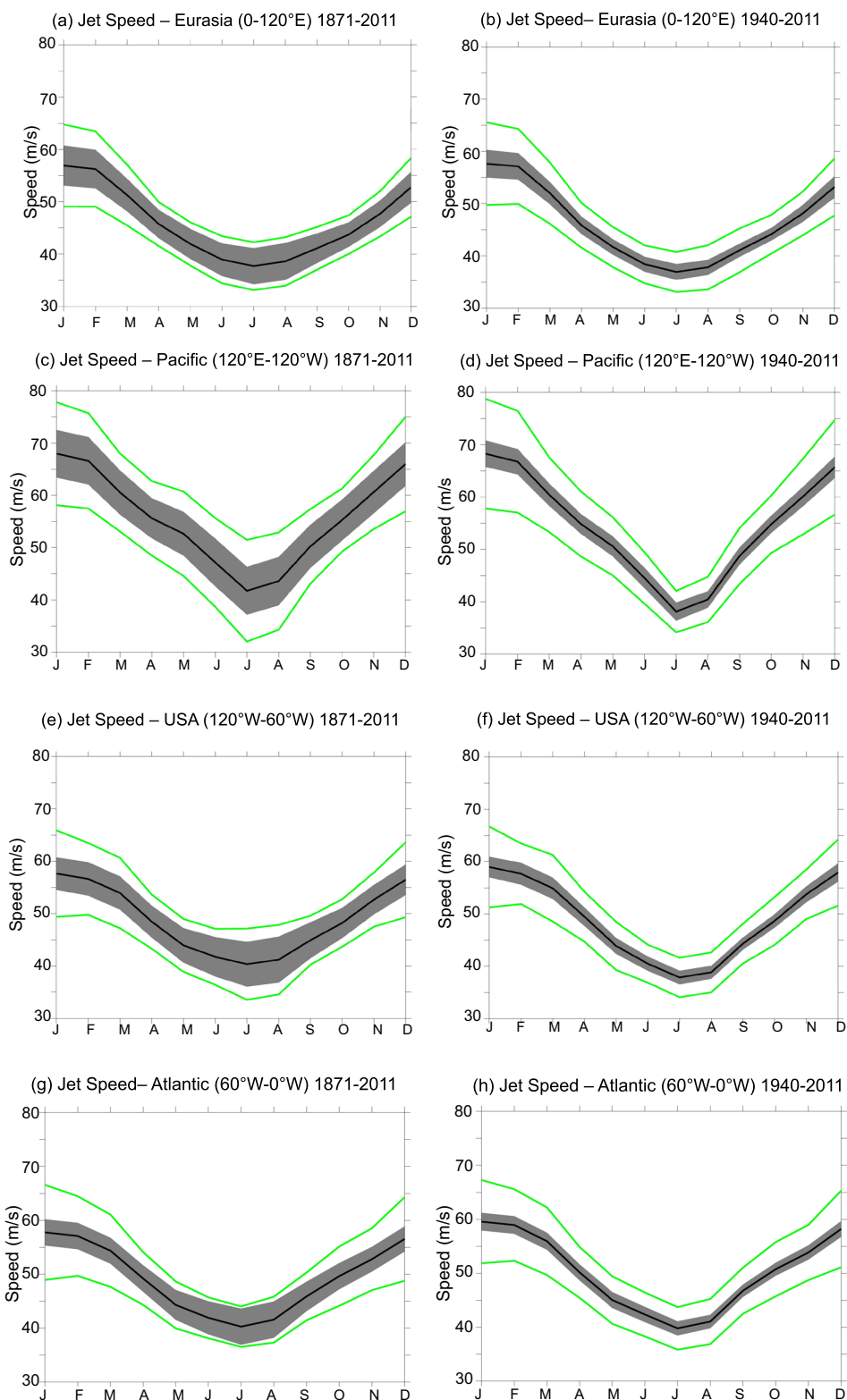
Of particular note is the narrow range in the mean jet latitude position in winter along the western boundary of the North Atlantic and North Pacific. The jet is located 1° to the north of the maximum gradient of the 2 m air temperature and is aligned with the temperature contours. The relationship between the mean jet position along the western boundary, and the maximum gradient of 2 m air temperature is retained in Spring and Autumn although not as tightly defined with the mean jet position located 3° and 4° north of the maximum gradient, respectively. The 2 m air gradient and land-sea temperature contrast are not as strong in these seasons. No relationship is evident in summer. It would perhaps be expected that the relationship of the maximum gradient of 2 m air temperature and mean jet latitude would also been seen over land. Although there is some relation, it is not as clear.

4.2 Multi-decadal trends in jet latitude and speed

This section details decadal trends for the Northern Hemisphere and then on a regional basis. *Significant trends are at the 95% confidence level or higher*. Jet latitude shows differing trends in each season (Fig. 6). For the northern hemisphere in winter (DJF) there is a significant 1.2° (0.1°/decade) long-term increase from a mean of 37.5 to 38.7° N (Fig. 6). In spring (MAM) there is no significant change in the mean of 44.3° N. In summer (JJA) only the trend after 1940 is considered, due to the range in the standard deviation in the earlier period. There has been a 0.3° N increase in jet latitude. In Autumn (SON) there is a significant 1° (0.1°/decade) decrease in the jet latitude from 49.4° N to 48.4° N over 141 years.

When trends are analysed on a regional basis, a different picture unfolds (Fig. 7). For winter (DJF) significant increasing trends in jet latitude are seen over the North Atlantic of 3.0° (0.2°/decade) from 44° N to 47° N and over Eurasia with an increase of 1.7°(0.1°/decade) from 33.1° N to 34.8° N. Across the North Pacific and North America there is no

**Fig. 4** Seasonal Jet Speed Climatology in the Northern Hemisphere by region for periods 1871–2011 (**a**, **c**, **e**, **g**) and 1940–2011 (**b**, **d**, **f**, **h**). Black line is mean jet speed. Grey area is ± 2 standard deviations smoothed over 31 days using a Parzen filter based on the 56 ensemble members. Green line is ± 2 standard deviations based on the interannual variability for the period

(a) Jet Speed – Eurasia (0-120°E) 1871-2011

(b) Jet Speed– Eurasia (0-120°E) 1940-2011

(c) Jet Speed – Pacific (120°E-120°W) 1871-2011

(d) Jet Speed – Pacific (120°E-120°W) 1940-2011

(e) Jet Speed – USA (120°W-60°W) 1871-2011

(f) Jet Speed – USA (120°W-60°W) 1940-2011

(g) Jet Speed– Atlantic (60°W-0°W) 1871-2011

(h) Jet Speed – Atlantic (60°W-0°W) 1940-2011

change in the mean position over the 141 year period. In Spring (MAM) only the North Atlantic shows a significant increasing trend in mean jet latitude of 1.8° (0.1°/decade) from 45.6 to 47.4° N (Supplementary Fig. 1). Over Eurasia

there is no change in the mean of 43.6° N. The Pacific and North America show a decreasing trend until the 1940s and increasing thereafter, but the increase is not statistically significant. For the summer (JJA) after 1940, only Eurasia has

Fig. 5 Mean Seasonal Jet Stream Position overlaying the 2 m air temperature for the period 1871–2011. The dark blue line indicates the mean jet stream position and the green line ± 2 standard deviations of the 6 hourly jet latitude smoothed over 91 days using a Parzen filter, for the period shown, based on the 56 ensemble members. The cyan blue line is ± 2 standard deviations of the 6 hourly jet latitude smoothed over 91 days using a Parzen filter, for the period shown, based on the interannual variability for the period. The jet stream overlays the seasonal average 2 m air temperature
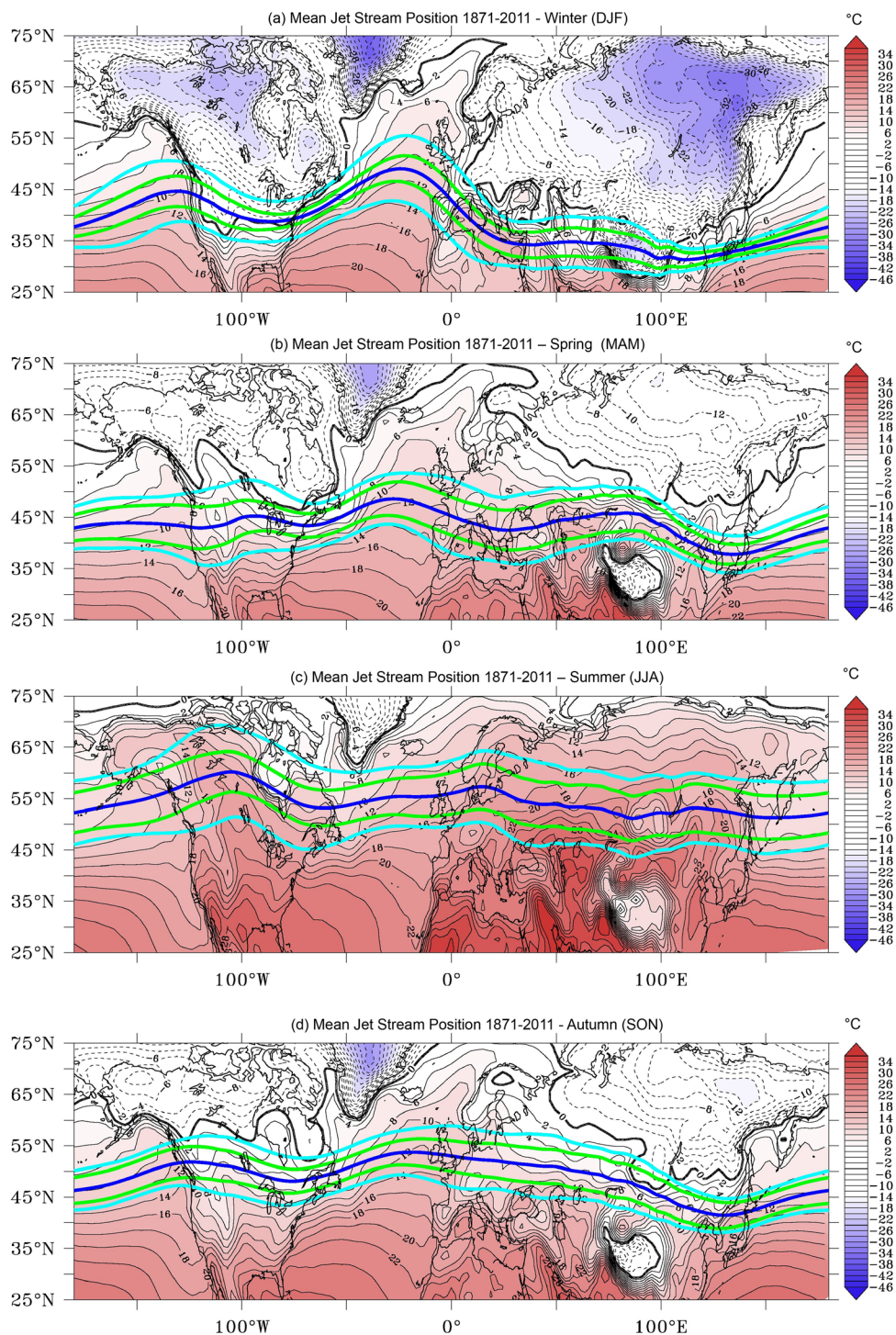
a significant increase of 1.6° (0.1°/decade) from 51 to 52.6° N (Supplementary Fig. 1). The North Atlantic has a modest 0.4° increase. The North Pacific and North America show a 0.3° and 1.2° decrease, respectively, but neither is statistically significant. In Autumn (SON) the North Atlantic is not in line with the hemisphere trend with an increase of 0.8° N, although not statistically significant (Supplementary Fig. 1). Eurasia has no change, whilst North America and the

North Pacific display a significant decreasing trend of 0.15°/ decade, however the trend becomes modest after 1940 and is not significant thereafter.

Overall, only the North Atlantic shows an increasing trend in jet latitude across all seasons. Eurasia shows significant increases but only in winter and summer, whilst the North Pacific and North America have either no change or decreases in the seasons.

Fig. 6 Northern Hemisphere Jet Latitude by season from 1871 to 2011. **a** Winter jet latitude (DJF). **b** Spring jet latitude (MAM). **c** Summer jet latitude (JJA). **d** Autumn jet latitude (SON). The thick black line indicates the seasonal mean. The red line indicates the seasonal mean with a Parzen filter smoothing over 11 years. The blue line indicates the 5-year running mean. The thin black lines indicate ±2 standard deviations based on the 6 hourly data for the 56 ensemble members smoothed over 91 days
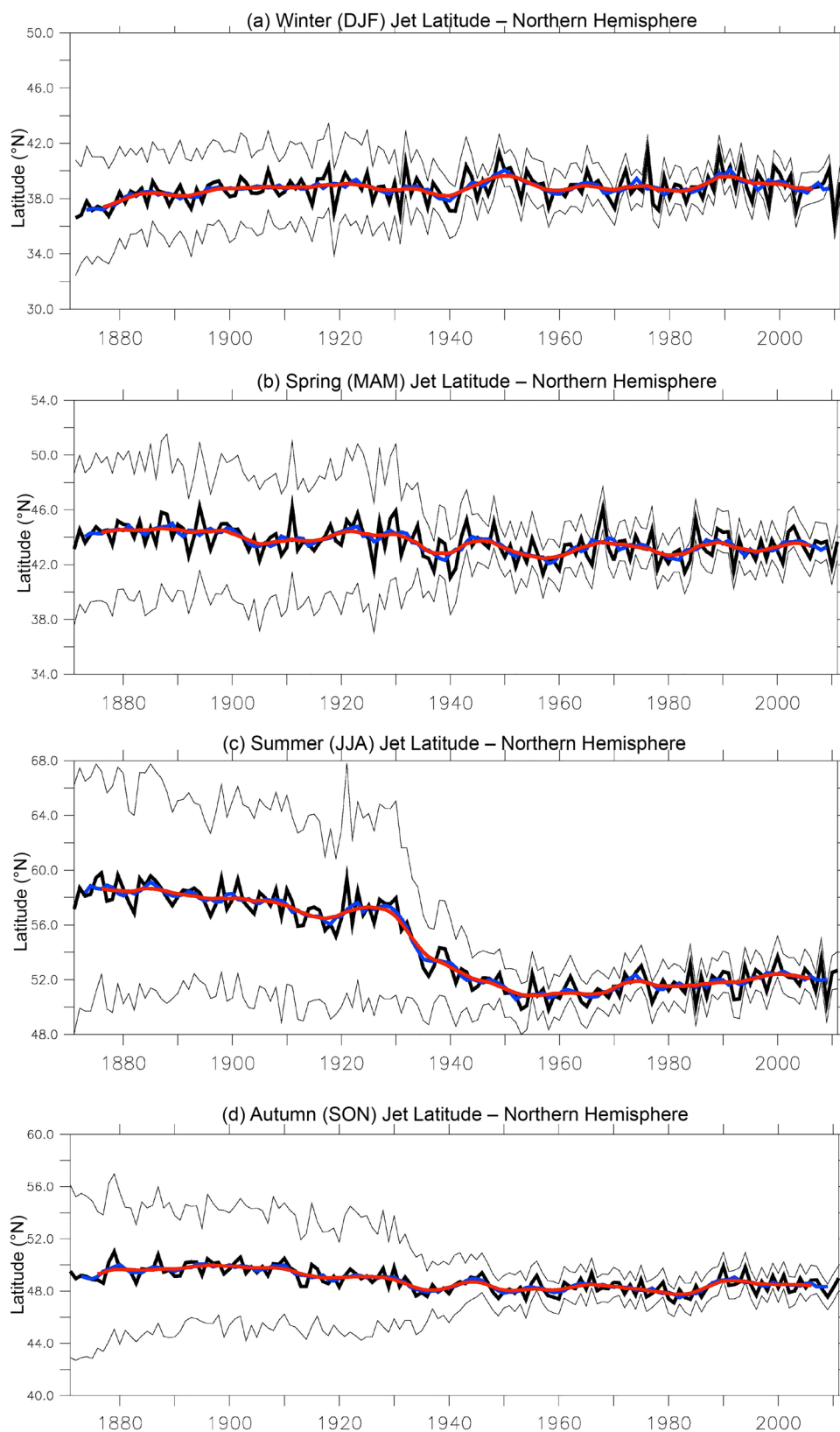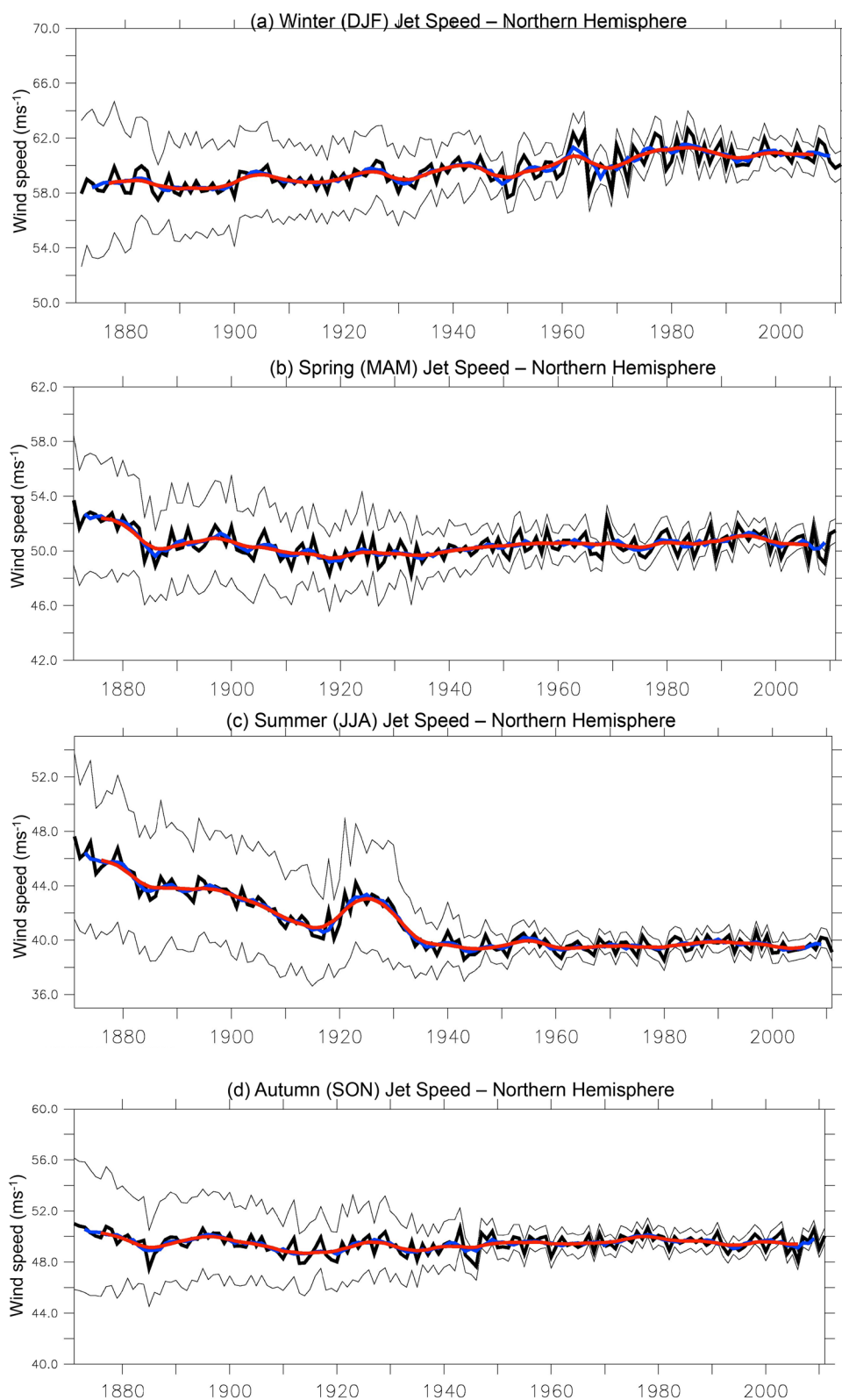

(a) Winter (DJF) Jet Latitude – Northern Hemisphere

(b) Spring (MAM) Jet Latitude – Northern Hemisphere

(c) Summer (JJA) Jet Latitude – Northern Hemisphere

(d) Autumn (SON) Jet Latitude – Northern Hemisphere

Fig. 7 Winter Jet Latitude by region from 1871 to 2011. The thick black line indicates the seasonal mean. The red line indicates the seasonal mean with a Parzen filter smoothing over 11 years. The blue line indicates the 5-year running mean. The thin black lines indicate ±2 standard deviations based on the 6 hourly data for the 56 ensemble members smoothed over 91 days
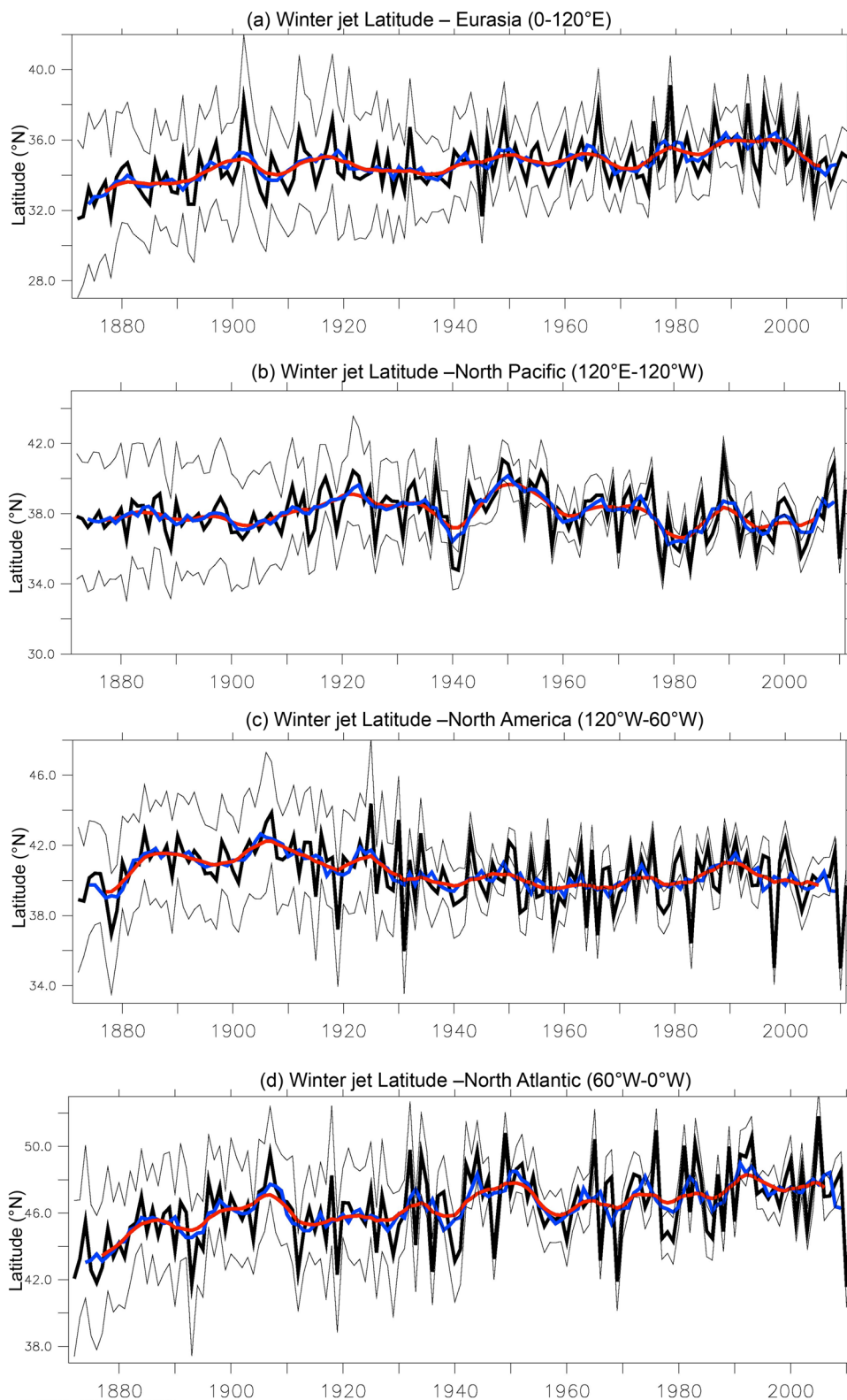
Jet speed shows a significant increase of 2.0 ms^{-1} for winter in the Northern Hemisphere (0.1 ms^{-1}/decade) (Fig. 8). In the other seasons, there is a decrease in jet speed from 1871 to 1940 followed by modest (not statistically significant) increase thereafter of between 0.1 and 0.3 ms^{-1}. Again, there are regional differences (Fig. 9 and Supplementary Fig. 2). In winter, we observe significant jet speed increases: North America 4.73 ms^{-1} (0.3 ms^{-1}/decade), the

Fig. 8 Jet Speed for the Northern Hemisphere from 1871 to 2011. **a** Winter jet speed (DJF). **b** Spring jet speed (MAM). **c** Summer jet speed (JJA). **d** Autumn jet speed (SON). The thick black line indicates the seasonal mean. The red line indicates the seasonal mean with a Parzen filter smoothing over 11 years. The blue line indicates the 5-year running mean. The thin black lines indicate ± 2 standard deviations based on the 6-hourly data for the 56 ensemble members smoothed over 91 days

(a) Winter (DJF) Jet Speed – Northern Hemisphere

(b) Spring (MAM) Jet Speed – Northern Hemisphere

(c) Summer (JJA) Jet Speed – Northern Hemisphere

(d) Autumn (SON) Jet Speed – Northern Hemisphere

North Atlantic 4.52 ms^{-1} (0.3 ms^{-1}/decade) and over Eurasia 1.8 ms^{-1} (0.1 ms^{-1}/decade). No trend is seen for the North Pacific. In spring, regional trends are in line with winter, with the largest significant increase seen over the North Atlantic (2.4 ms^{-1}, 0.2 ms^{-1}/decade), and speed increases of 1 ms^{-1} (0.1 ms^{-1}/decade) over North America and Eurasia.

Fig. 9 Winter Jet Speed by region from 1871 to 2011. The thick black line indicates the seasonal mean. The red line indicates the seasonal mean with a Parzen filter smoothing over 11 years. The blue line indicates the 5-year running mean. The thin black lines indicate ± 2 standard deviations based on the 6-hourly data for the 56 ensemble members smoothed over 91 days
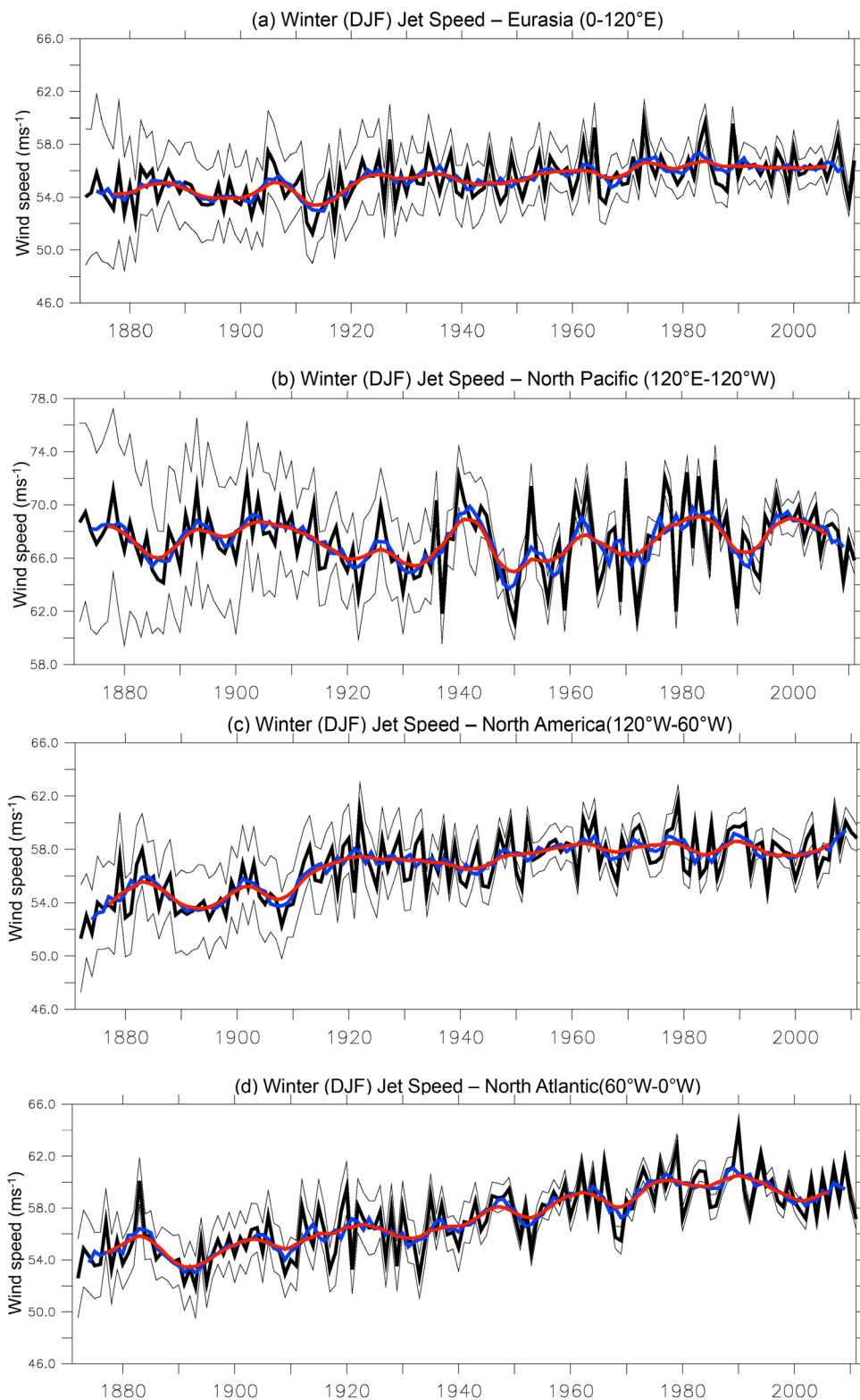
In summer, only the period after 1940 is considered. A significant increasing trend is seen over North America of 1.6 ms^{-1} (0.2 ms^{-1}/decade). For autumn; the North Atlantic has a significant 3 ms^{-1} (0.2 ms^{-1}/decade) increase,

North America a 1.2 ms^{-1} (0.2 ms^{-1}/decade) increase for the period since 1940, but no change over the full period. Across Eurasia the increasing trend seen is not significant after 1940. Over the Pacific, the decadal jet speed trends are

different. In winter, as with jet latitude, there is no change in the mean jet speed of 67.7 ms^{-1} but there is significant inter-annual variability from 62 to 72 ms^{-1}. In the other seasons, there are no significant trends since the 1940s.

The extent of the relationship between jet latitude and speed was also evaluated for each region and season (Table 1). Over the North Pacific there is a significant nega-tive correlation in all seasons, which is strongest in winter, explaining 42% of the variance. The highest negative cor-relation is located in the eastern part of the North Pacific at 170° W, explaining 64% of the variance since 1940 (not shown). Over North America, a significant negative cor-relation exists in spring and autumn. Over the North Atlan-tic there is a positive correlation in winter and spring, but negative in summer and autumn. The strongest significant correlation was in winter, for the period 1871–2011, but only explains 9% of the variance. Woollings et al. (2014) also show a low correlation between jet latitude and speed over the North Atlantic. On closer analysis of the North Atlantic in winter, however, there is a negative correlation west of 40° W (maximum value at 60° W r = − 0.3) and positive cor-relation 40° W to 0° W (maximum value at 10° W, r = 0.5), which is masking the true picture for the region. We note that the eastern Atlantic is the only region where significant positive correlations are found between jet stream latitude and speed.

4.3 Interannual to decadal variability of jet latitude and speed

The interannual to decadal variability seen in Figs. 3, 4, 6 and 7 is analysed in more detail using wavelet analysis and compared to known atmospheric and ocean indices; Atlantic Multidecadal Oscillation (AMO), North Atlantic Oscillation (NAO), Pacific Decadal Oscillation (PDO) to investigate if any co-variability exists on decadal timescales. The Atlantic Multidecadal Oscillation (AMO) Index, is defined as the area average SST anomaly over the North Atlantic (0° N–65° N, 80° W–0° E). It is usually detrended to show only interan-nual variability and has a periodicity of around 65–70 years (Schlesinger and Ramankutty 1994). Warm phases have occurred from 1930–1965 and since 1995 with cool phases of the AMO between 1900–1930 and 1965–1995. The lin-early detrended AMO index was correlated with the North Atlantic jet latitude and jet speed. For jet latitude and jet speed significant positive correlations were observed in winter (summer) with r = 0.24 (r = 0.32) for jet latitude and r = 0.28 (r = 0.3) for jet speed. The low correlation is similar to the winter findings by Woollings et al. (2014).

The NAO is an atmospheric index based on the surface sea level pressure (SLP) difference between the subpolar (Icelandic) low and the subtropical (Azores) high. During a positive (negative) phase of the NAO there is a greater (smaller) difference between the SLP between the Azores high and the Icelandic low (Hurrell 1995). The PDO index (Mantua and Hare 2002) is the leading empirical orthogonal function (EOF) of monthly SSTA over the North Pacific (poleward of 20° N) after the global SST has been removed, with 2 periodicities; 15–25 years and 50–70 years. We use wavelet cross-coherence to identify the links between jet latitude/speed and the PDO/NAO (Torrence and Compo 1998). Correlations between NAO/PDO and jet stream lati-tude/speed over the Atlantic and Pacific regions are shown in Table 2.

Table 1 Jet Latitude and Jet Speed Correlation (r) for the periods 1940–2011 (1871–2011) Statistically significant correlations at the 95% confidence level or higher are shown in bold

	DJF	MAM	JJA	SON
Eurasia	**− 0.24** (− 0.08)	0.08 (− 0.01)	− 0.18 (n/a)	0.06 (**− 0.18**)
North Pacific	**− 0.65 (− 0.65)**	**− 0.56** (0.10)	**− 0.39** (n/a)	**− 0.40** (0.14)
North America	− 0.15 (0.15)	**− 0.46 (− 0.50)**	− 0.18 (n/a)	− 0.15 (**− 0.23**)
North Atlantic	0.02 (**0.30**)	0.16 (**0.24**)	**− 0.46** (n/a)	− 0.05 (**− 0.21**)

Table 2 Jet Latitude and Jet Speed Correlation (r) with the NAO/PDO 1940–2011 (1871–2011) Statistically significant correlations at the 95% confidence level or higher are shown in bold

	DJF	MAM	JJA	SON
North Atlantic and NAO				
Latitude	**0.57** (0.45)	**0.28** (0.30)	− 0.24 (n/a)	− 0.18 (**− 0.18**)
Speed	**0.23** (0.18)	**0.46** (0.44)	0.15 (n/a)	**0.40** (0.38)
North Pacific and PDO				
Latitude	**− 0.71 (− 0.62)**	**− 0.51 (− 0.44)**	**− 0.38** (n/a)	**− 0.46 (− 0.32)**
Speed	**0.53** (0.45)	**0.46** (0.42)	0.16 (n/a)	− 0.02 (0.11)

When looking at the PDO/NAO we find that the links with the jet stream latitude and speed vary greatly between regions and seasons. Over the North Pacific, jet latitude and PDO are in antiphase (Table 2; Fig. 10) and in winter show continuous significant coherence for periods between 12 and 30 years. Jet Speed and the PDO are in phase (Table 2; Fig. 11) and in winter show continuous significant coherence between 12 and 26 years.

Over the North Atlantic in winter, jet latitude and NAO are in phase and show significant coherence at 20-year timescales for the period 1930–1960 (Fig. 10), and significant coherence at 8–10 year timescales for the period since 1980. Jet speed and the NAO are in phase and in spring show significant coherence at 16–24 year timescales for the period since 1940 (Fig. 11). Over Eurasia, in the transition seasons of spring and autumn, jet latitude and the NAO
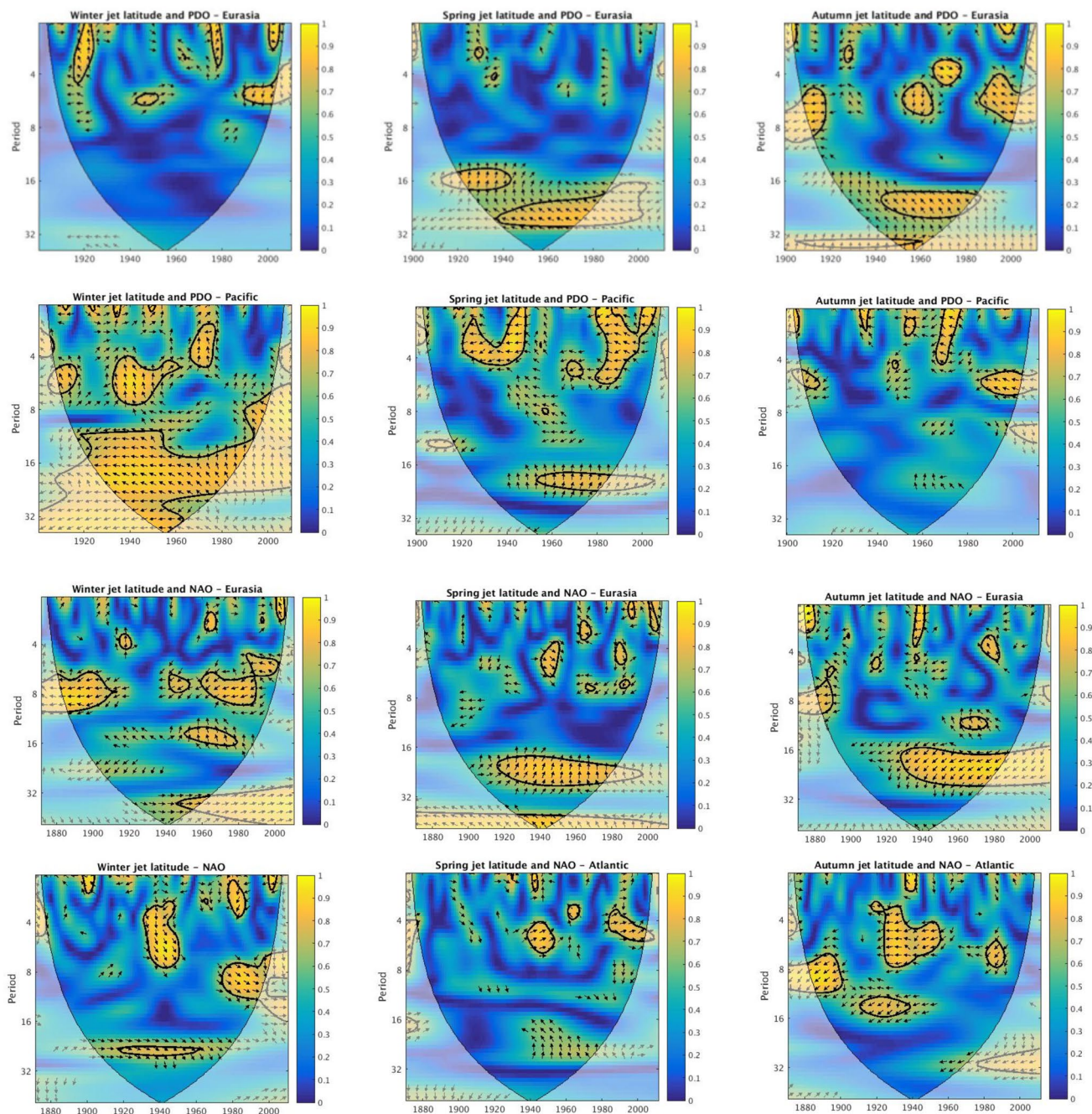
Fig. 10 Wavelet coherence for Jet Latitude by region. Colour bar indicates correlation. Black contours indicate statistically significant features (95% confidence level)
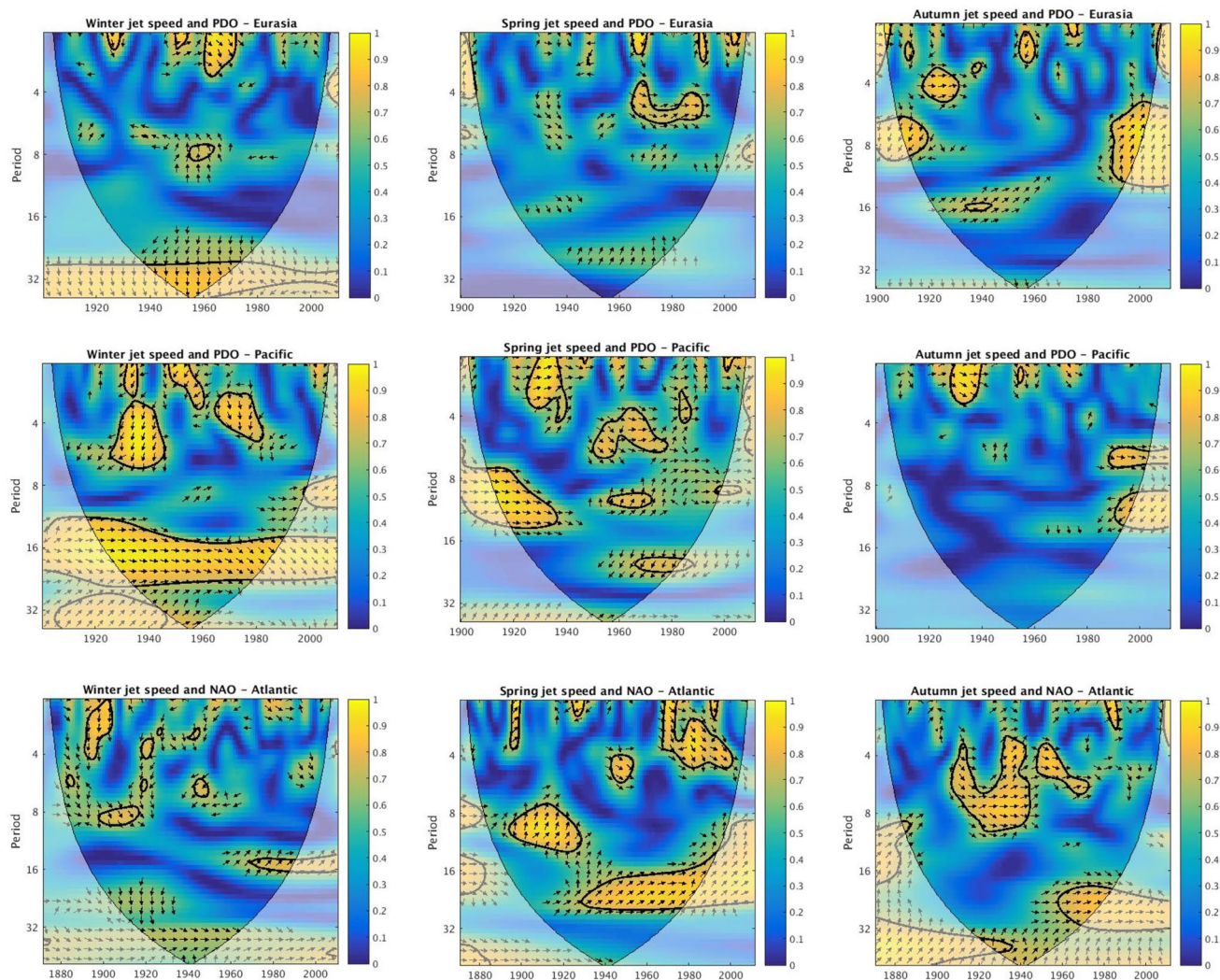
Fig. 11 Wavelet coherence for Jet Speed by region. Colour bar indicates correlation. Black contours indicate statistically significant features (95% confidence level)

show significant coherence since the 1930s on timescales of 16–28 years (Fig. 10), whilst jet latitude and the PDO are out of phase over Eurasia and show significant coherence at timescales of 20–28 years (Fig. 10). Winter jet speed and the PDO are in phase and show significant coherence at timescales of 28–40 years (Fig. 11).

The clearest relations occur over the North Pacific during the winter season where 50% of the variance in North Pacific winter jet latitude variability and 28% of the winter jet speed variance is explained through the correlation with the PDO index since 1940 on timescales of about 20 years (Figs. 10, 11). The coherence between the jet latitude/speed and the PDO occurs for periods of about 20 years which are consistent with one of the dominant timescales of the PDO (Mantua and Hare 2002). The correlation between the PDO and the jet latitude over the Pacific domain is substantially weaker during spring and autumn but over Eurasia we find a

significant cross coherence between the PDO and jet latitude (Fig. 10), this contrasts with the winter season when the cross-coherence between PDO and the jet latitude is strongest over the Pacific but we find no relationship over Eurasia (Fig. 10).

An interesting aspect emerging from Figs. 10 and 11 is that an apparent link between the PDO and the jet stream is not confined to the Pacific but is also seen over Eurasia. In contrast to the Pacific, the strongest coherence with jet latitude is not found in winter but during spring and autumn. As for the PDO we find significant cross wavelet correlations between the NAO and the jet latitude over Eurasia during spring and autumn for periods of around 20 years but not for winter. Given the large spatial scales of both the PDO and the NAO one could expect these modes of variability to affect the jet stream over Eurasia. So why is this cross correlation not seen during winter when the cross-coherence

between jet and PDO (NAO) is strongest over the Pacific (Atlantic)?

For an explanation we look at the seasonal evolution of the Siberian High (SH) and of the related cold air pool. The SH is the strongest centre of action on the Northern Hemisphere during winter. Most pronounced in winter it is also present—albeit weaker—during spring and autumn and only vanishes in summer (Fig. 12). In autumn and spring, the SH expands and wanes. The pool of cold air linked to the SH develops from September onwards in Yakutia and the Baikal region from where it gradually spreads westward reaching its full extent in January. The SH is an extremely persistent winter feature around which the jet stream has to swerve. Even though the strength of the SH varies on interannual timescales, this variability is small compared to the average winter SH strength. This is illustrated with the ratio R_i in Fig. 12. R_i is a measure of the average strength of surface level pressure features with respect to their interannual variability:

$$R_i = \frac{\left| \langle SLP_i \rangle - \overline{\langle SLP_i \rangle} \right|}{\sqrt{\frac{1}{n} \sum_{j-1}^{n} \left(SLP_{ij} - \langle SLP_i \rangle \right)^2}}, \, i = [1, \ldots, 12]$$

$$\overline{\langle SLP_i \rangle} = \frac{1}{2\pi} \int\limits_{0}^{2\pi} \langle SLP_i \rangle d\vartheta$$

$$\langle SLP_i \rangle = \frac{1}{n} \sum_{j=1}^{n} SLP_{ij}$$

where SLP_{ij} is the sea level pressure for month i in the year j, $< >$ denote the time average for the month i over the 1871–2011 period and the overbar denotes the zonal average (ϑ is the azimuth).

During the winter season the highest ratio R_i occurs over eastern Siberia over the south-eastern SH. What the high values of R_i over eastern Siberia in winter suggest is that even in years when the SH is very weak the pressure over eastern Siberia remains higher than at the adjacent regions further south. With R_i around 5 (Fig. 12, top) the SH is more stable than any of the other centres of action of the Northern Hemisphere in winter (Icelandic Low, Aleutian Low, North American High). Note that the maximum values of the ratio R_i on the Northern Hemisphere in spring and summer can exceed the winter maxima seen over Siberia. However, these values occur along the south-eastern flanks of the Azores and Pacific Highs as well as over the low pressure area over Southern Asia linked to the Asian Monsoon. All these features are located well south of the jet stream position for these seasons (Fig. 5) and hence do not constrain the jet stream path like the SH in winter.

5 Discussion

This study highlights that the jet variability, on seasonal to decadal timescales, is different in each region; North Atlantic, North Pacific, Eurasia and North America. Although some similarities exist, the significant differences suggest

Fig. 12 Sea level pressure (SLP) for each season minus the zonally averaged SLP for that season (contours). Shading shows the ratio R_i for DJF, MAM, JJA, SON (from top to bottom). Units are hPa
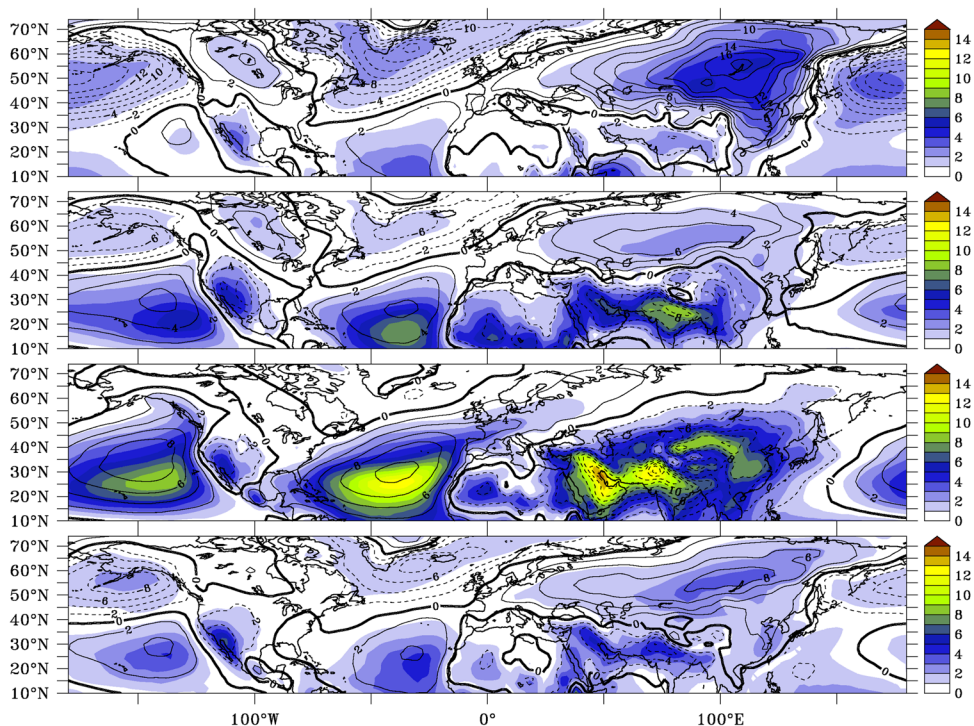
separate mechanisms are modulating the jet latitude and speed behaviour, which are now discussed in more detail.

5.1 Seasonal jet climatology

Over the oceans, particularly the North Atlantic, the annual range in jet latitude is significantly lower. This is linked to the lower variability in the seasonal 2 m air temperature over the oceans, which is due to the greater heat capacity of the oceans of 6×10^{24} J K^{-1} compared to the atmosphere of 5×10^{21} J K^{-1} (Levitus 1983). The larger oceanic heat capacity results in an accumulation of heat in the mid-latitude oceans during the summer, which is released during the winter months and reduces the overlying temperature range. Compared to North America and Eurasia, the seasonal cycle of the jet latitude is lagged over the North Atlantic and Pacific and the maximum/minimum is reached in September and March, respectively. These findings are similar to Woollings et al. (2014) with a peak maximum latitude in September over the North Atlantic, although Woollings et al. (2014) show a seasonal range in latitude of 5° compared to the 10° (7° for the period 1940–2011) found in this study, perhaps related to the different pressure heights analysed, 850 mb versus 250 mb here. Czaja (2009) found the mean jet stream latitude to be 48° N for the North Atlantic, with a standard deviation of 7° for the period 1980–2005. It is important that models replicate jet seasonality correctly in order to simulate seasons realistically. Harvey et al. (2020) found that jet stream biases have improved in the CMIP 6 models (compared to CMIP 5) over the Atlantic but still place the jet stream too far south in winter therefore overestimating the seasonal cycle. Little improvement in the biases has been seen over the Pacific where there is an equatorward bias in winter.

The seasonal jet stream range is much smaller over the North Atlantic than over the North Pacific. A key difference between these basins is the poleward meridional heat transport (MHT) by the oceans. In the Atlantic sector the oceanic MHT is positive at all latitudes and there is a net MHT across the equator (Trenberth and Caron 2001). The Atlantic MHT reaches a maximum of 1.3 PW at 25° N, associated with the Atlantic Meridional Overturning Circulation (AMOC) (Johns et al. 2011). The oceanic MHT poleward in the Pacific is lower at 0.76PW at 25° N (Bryden et al. 1991) and is predominantly poleward in the Northern and Southern Hemispheres (Trenberth and Caron 2001). The stronger oceanic MHT in the Atlantic leads to SSTs up to 4 °C warmer at similar latitudes in the Atlantic than in the Pacific (Levitus 1983), and decreases the poleward temperature gradient resulting in a reduced atmospheric MHT, in line with the Bjerknes compensation (van der Swaluw et al. 2007). These results suggest that oceanic MHT changes may impact the seasonal variations in the jet latitude, but further research

on this hypothesis would be required to confirm this. The tightly defined winter mean jet stream position across the western boundary of the North Atlantic and North Pacific (Fig. 5) in the region where 2 m air temperature and SST gradients are strongest is in line with the studies by O'Reilly and Czaja (2015) for the western Pacific and in the North Atlantic by Feliks et al. (2016), O'Reilly et al. (2016) and Fang and Yang (2016). What is important here is that the findings over shorter periods of time and 850 mb are confirmed in this study over 141 years and at 250mb, and also show the interannual variability over that period.

## 5.2 Multi-decadal trends in jet latitude and speed

For the Northern hemisphere as a whole, there is a significant 0.1°/decade increase in jet latitude in winter, no significant trend in spring or summer and a significant 0.1°/decade decrease in autumn which is in line with the seasonal findings by Pena-Ortiz et al. (2013) using the same data but their winter and autumn trends were not significant, due to the shorter period analysed.

On a regional basis, however, the long-term trend from 1871 to 2011 in jet latitude is not uniform. Only the North Atlantic shows an increasing trend across all seasons, with a maximum increase seen in winter of 3.0° (0.2°/decade), which is in agreement with Woollings et al. (2014). Eurasia shows significant increases but only in winter (1.5°, 0.1°/decade), in line with Strong and Davis (2007), and summer (1.6°, 0.1°/decade), where the increase is greater than for the North Atlantic. Over the North Pacific and North America there is either no change or decreases over the seasons. Strong and Davis (2007) also found no change in winter jet latitude in the west and central North Pacific for the period 1958–2007. Again, the multi-decadal trends in jet latitude over shorter periods are confirmed by this study.

Two broad jet latitude patterns have emerged; increasing trends over the North Atlantic and Eurasia and flat/decreasing trends over the North Pacific and North America. The increasing jet latitude trends seen over the North Atlantic and Eurasia are in line with other northern hemisphere research by Woollings et al. (2014) and Pena-Ortiz et al. (2013), and consistent with a decreasing temperature gradient between the poles and the equator at the tropopause, as highlighted in Fig. 13.

On a decadal basis, in line with the seasonal results, it appears that different mechanisms are impacting jet latitude in the North Pacific compared to the North Atlantic. This is consistent with results by Harvey et al. (2014) who found, in the CMIP5 models, that the North Atlantic winter time storm track was sensitive to equator to pole temperature differences, but suggest other mechanisms such as changes to the zonal structure of the Tropical Pacific SSTs may influence the North Pacific storm track. Kuang et al. (2014) also found

Fig. 13 Northern Hemisphere temperature difference at the Tropopause (upper panel) and 300mb Geopotential Height Difference (lower panel) between the equator (0–20° N) and North Pole (70–90° N) for the period 1871–2011. Pink line indicates winter (DJF), Green line spring (MAM), Blue Line summer (JJA), Black line autumn (SON)
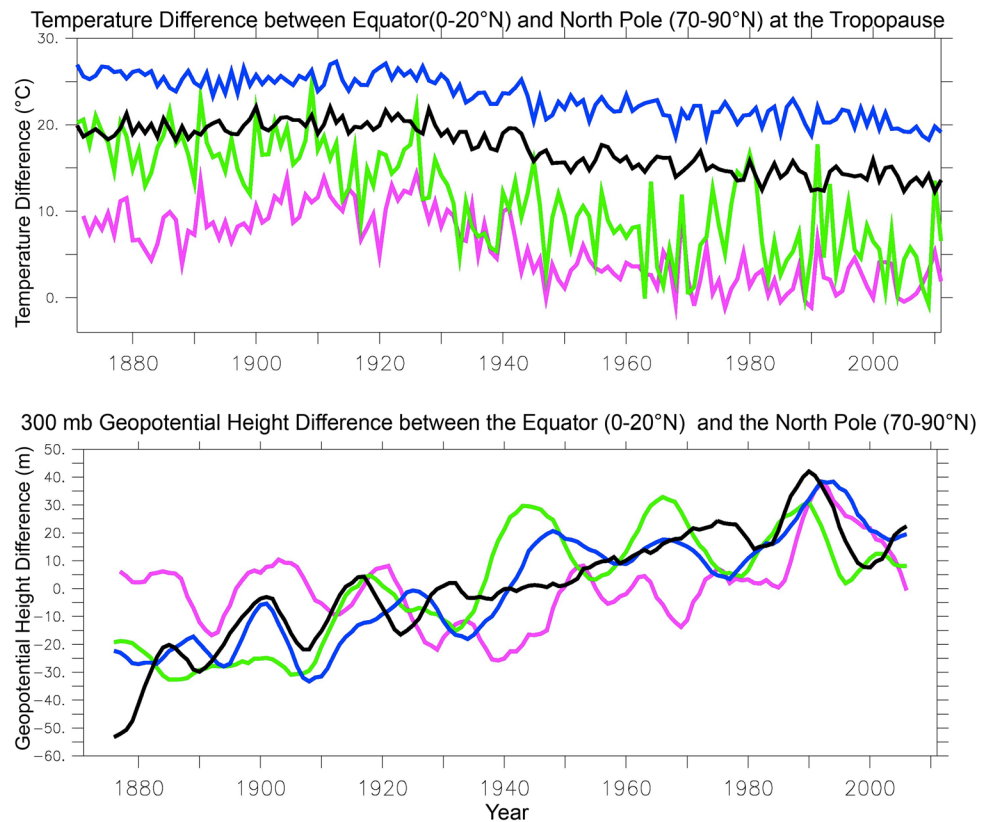
that the jet variability was sensitive to temperature gradients and baroclinicity over the Atlantic, whereas eddy heat and momentum transport were important over the Pacific.

For the whole northern hemisphere there has been a significant 0.1 ms^{-1}/decade increase in jet speed in winter, which is lower than the significant findings by Pena-Ortiz et al. (2013) using the NCEP/NCAR data for the shorter period (1958–2008 and 1979–2008). For the other seasons, a decrease was seen from 1871 to 1940 and very modest increases thereafter, which are not significant. The findings are in agreement with Pena-Ortiz et al. (2013) using the 20CR data, but lower than the increasing trends in speeds seen using NCEP/NCAR data for the shorter period.

The regional trends, however, show that increases are seen in winter, spring and autumn in the North Atlantic, Eurasia and North America, many of which are significant and up to 0.3 ms^{-1}/decade in winter. These findings are consistent with the Pena-Ortiz et al. (2013) results using the NCEP/NCAR data.

The North Pacific region shows no change in winter jet speed and decreasing trends in the other seasons for the period 1871–2011. At first it appears this is not in agreement with Strong and Davis (2007) who find an increasing trend in winter jet latitude over the North Pacific of up to 1.75 ms^{-1}/decade at 35° N between 1958 and 2007. If we refine our study, however, to the same period (1958–2007) we also find an increase in winter jet speed. It appears the increase

between 1958 and 2007 is perhaps multidecadal variability in the context of the longer time period, 1871–2011 rather than a long-term trend.

The increasing northern hemisphere and regional trends in jet speed are consistent with changes in the 300mb geopotential height gradient between the equator and the North Pole, where there is an increasing trend of up to 50 m in each season (Fig. 13), which would be expected to lead to an increase in jet speed. The regional exception is over the North Pacific (not shown), where there is a decreasing trend in geopotential height gradient in winter and increasing trend in the other seasons, which is not consistent with the wind speed trends observed.

Overall, the similarity of the jet latitude findings with other studies helps to confirm the trends observed in studies over shorter timescales. For jet speed, care in needed with suggested trends observed over the North Pacific on short timescales as significant interannual variability is observed, as evident for the period 1871–2011. A trend may just be part of the overall multidecadal variability.

5.3 Interannual to decadal variability

Interannual variability is most evident in the North Pacific, where 50% of the variance in North Pacific winter jet latitude variability and 28% of the winter jet speed variance is

explained through the correlation with the PDO index since 1940 (Figs. 10, 11; Table 2). There is a negative correlation with jet latitude and positive correlation with jet speed.

The correlation is consistent with the ocean changes during the different PDO phases. During a positive (negative) PDO phase there is an increased (decreased) meridional temperature gradient in the North Pacific; which is anomalously warm (cold) at low latitudes and colder (warmer) than normal north of the Kuroshio extension. The increase (decrease) in the meridional temperature gradient is conducive to a southward (northward) shift in the jet stream and stronger (weaker) winds over the north Pacific region. The findings here are consistent with Sung et al. (2014) who also find that both the jet stream and storm track move northward (southward) over the North Pacific during negative (positive) PDO winters.

The link between the PDO and the jet stream is not, however, confined to the Pacific but is also seen over Eurasia with the strongest coherence with jet latitude during spring and autumn. We find no link between the PDO and jet stream over Eurasia in Winter which we attribute to the strength of the Siberian High during that season. As the jet stream follows the southern flank of the SH it has to make a southward excursion taking it to the southernmost latitudes of its path around the globe. The stability of the SH is reflected in the jet stream path and Fig. 5 shows that nowhere else the jet stream is as tightly confined with by far the lowest temporal (and cross ensemble) variability. The stability of the SH and of the jet stream over East Asia can explain why the cross wavelet correlation seen between the PDO and the jet stream during winter over Eurasia (Fig. 10) is so low: no matter what the state of the PDO, NAO or indeed any other atmospheric mode of variability, the SH always dominates the winter pressure pattern over East Asia leading to similar average jet stream paths in most winters. During the transitional seasons of spring and autumn, however, the SH is weaker (albeit still present, see Figs. 10 and 12, 2nd and bottom panels) and modes of variability such as the PDO and the NAO start to compete with the SH in terms of influence on the jet stream path.

6 Conclusions

This study has shown it is helpful to undertake jet latitude and speed studies on a regional basis, to complement analyses covering the whole northern hemisphere, as regional trends and magnitudes may cancel out and therefore not be visible when averaged across the whole hemisphere.

The key new findings of this study are that substantial regional differences are seen for jet latitude and speed variability on seasonal to decadal timescales—particularly when comparing land and ocean regions.

Over the oceans the seasonal jet latitude range is reduced. This is particularly the case over the North Atlantic, where the oceanic MHT is greatest, and a 10° seasonal latitude range is seen, compared to a 20° range over land. Also, on a seasonal basis, the winter jet variability is more tightly confined over the western boundary of the North Pacific and North Atlantic over the 141-year period. This is the location where the land-sea contrast and SST gradients are strongest.

The North Pacific has significant interannual to decadal variability in jet latitude and speed associated with the PDO. In winter there is continuous significant cross-coherence on timescales of 12–30 years with the PDO, explaining 50% of the variance in winter jet latitude since 1940. A significant cross-coherence for periodicities around 20 years is also found between the PDO and the jet latitude over Eurasia during spring and autumn but not during winter. The absence of any clear link during winter is likely due to the winter strength of the Siberian high which prevents the PDO (or the NAO) from modulating the jet stream position.

Multidecadal increases in jet latitude are found in the North Atlantic in all seasons (0.2°/decade in winter). The trends vary significantly on a regional basis. Over Eurasia increases are seen in winter and summer (0.1°/decade), but no increasing trends are seen over the North Pacific and North America.

Multidecadal increases in jet speed are found in winter, spring and autumn over the North Atlantic, Eurasia and North America. The increasing trends are consistent with the changes in the geopotential height gradients over the period and region. Over the North Pacific no significant change in jet speed has been found in any season after 1940. The differing trends in jet latitude and speed between the North Atlantic and North Pacific, on seasonal to decadal timescales, suggest different mechanisms are operating in these areas.

The jet stream is key to mid-latitude weather and climate and the results suggest different jet stream behaviours and variability on seasonal to decadal timescales for different regions which has implications for models used for climate and weather predictions. To simulate a realistic climate, models would need to be able to reproduce the regional characteristics of the jet stream and interannual variability. An inability to do so (in a statistical sense) would cast doubt on the ability of such a model to generate reliable prediction of regional weather and climate patterns.

Declarations

Conflict of interest The authors declare no competing interest.

References

Anderson JL, Wyman B, Zhang S, Hoar T (2005) Assimilation of surface pressure observations using an ensemble filter in an idealized global atmospheric prediction system. J Atmos Sci 62:2925–2938

Archer CL, Caldeira K (2008) Historical trends in the jet streams. Geophys Res Lett 35

Barnes EA, Simpson IR (2017) Seasonal sensitivity of the Northern Hemisphere jet streams to arctic temperatures on subseasonal time scales. J Clim 30:10117–10137

Barry RG, Chorley RJ (2009) Atmosphere, weather and climate. Routledge, USA

Bryden HL, Roemmich DH, Church JA (1991) Ocean heat transport across 24°N in the Pacific. Deep Sea Research Part A. Oceanogr Res Pap 38:297–324

Compo GP, Whitaker JS, Sardeshmukh PD (2006) Feasibility of a 100-year reanalysis using only surface pressure data. Bull Am Meteor Soc 87:175–190

Compo GP, Whitaker JS, Sardeshmukh PD, Matsui N, Allan RJ, Yin X, Gleason BE, Vose RS, Rutledge G, Bessemoulin P, Brönnimann S, Brunet M, Crouthamel RI, Grant AN, Groisman PY, Jones PD, Kruk MC, Kruger AC, Marshall GJ, Maugeri M, Mok HY, Nordli Ø, Ross TF, Trigo RM, Wang XL, Woodruff SD, Worley SJ (2011) The twentieth century reanalysis project. Q J R Meteorol Soc 137:1–28

Czaja A (2009) Atmospheric control on the thermohaline circulation. J Phys Oceanogr 39:234–247

Czaja A, Blunt N (2011) A new mechanism for ocean–atmosphere coupling in midlatitudes. Q J R Meteorol Soc 137:1095–1101

Fang J, Yang X-Q (2016) Structure and dynamics of decadal anomalies in the wintertime midlatitude North Pacific ocean–atmosphere system. Clim Dyn 47:1989–2007

Feliks Y, Ghil M, Robertson AW (2011) The atmospheric circulation over the north Atlantic as induced by the SST Field. J Clim 24:522–542

Feliks Y, Robertson AW, Ghil M (2016) Interannual variability in north Atlantic weather: data analysis and a quasigeostrophic model. J Atmos Sci 73:3227–3248

Ferguson CR, Villarini G (2014) An evaluation of the statistical homogeneity of the Twentieth Century Reanalysis. Clim Dyn 42:2841–2866

Fu Q, Lin P (2011) Poleward shift of subtropical jets inferred from satellite-observed lower-stratospheric temperatures. J Clim 24:5597–5603

Gan B, Wu L (2013) Seasonal and long-term coupling between wintertime storm tracks and sea surface temperature in the north Pacific. J Clim 26:6123–6136

Gan B, Wu L (2014) Feedbacks of sea surface temperature to wintertime storm tracks in the north Atlantic. J Clim 28:306–323

Hartmann D, Kleinank A, Rusticucci M, Alexander L, Brönnimann S, Charabi Y, Dentener F, Dlugokencky E, Easterling D, Kaplan A, Soden B, Thorne P, Wild M, Zhai P (2013) Observations: atmosphere and surface. In climate change 2013 the physical science basis: working group I contribution to the fifth assessment report of the intergovernmental panel on climate change. Cambridge University Press, Cambridge

Harvey BJ, Shaffrey LC, Woollings TJ (2014) Equator-to-pole temperature differences and the extra-tropical storm track responses of the CMIP5 climate models. Clim Dyn 43:1171–1182

Harvey BJ, Cook P, Shaffrey LC, Schiemann R (2020) The response of the northern hemisphere storm tracks and jet streams to climate change in the CMIP3, CMIP5, and CMIP6 climate models. J Geophys Res Atmos 125:2020032701

Holton JR (1992) An introduction to dynamic meteorology 3rd ed. International geophysics series, vol 23. Academic Press, Cambridge, p 511

Hoskins BJ, Valdes PJ (1989) On the existence of storm-tracks. J Atmos Sci 47:1854–1864

Hurrell JW (1995) Decadal trends in the north atlantic oscillation: regional temperatures and precipitation. Science 269:676

Iqbal W, Leung W-N, Hannachi A (2018) Analysis of the variability of the North Atlantic eddy-driven jet stream in CMIP5. Clim Dyn 51:235–247

Johns WE, Baringer MO, Beal LM, Cunningham SA, Kanzow T, Bryden HL, Hirschi JJM, Marotzke J, Meinen CS, Shaw B, Curry R (2011) Continuous, array-based estimates of atlantic ocean heat transport at 26.5° N. J Clim 24:2429–2449

Koch P, Wernli H, Davies HC (2006) An event-based jet-stream climatology and typology. Int J Climatol 26:283–301

Kuang X, Zhang Y, Huang Y, Huang D (2014) Spatial differences in seasonal variation of the upper-tropospheric jet stream in the Northern Hemisphere and its thermal dynamic mechanism. Theoret Appl Climatol 117:103–112

Lee S, Kim H (2003) The dynamical relationship between subtropical and eddy-driven jets. J Atmos Sci 60:1490–1503

Levitus S (1983) Climatological atlas of the world ocean. Eos Trans Am Geophys Union 64:962–963

Manney GL, Hegglin MI (2018) Seasonal and regional variations of long-term changes in upper-tropospheric jets from reanalyses. J Clim 31:423–448

Mantua NJ, Hare SR (2002) The pacific decadal oscillation. J Oceanogr 58:35–44

Minobe S, Kuwano-Yoshida A, Komori N, Xie S-P, Small RJ (2008) Influence of the Gulf Stream on the troposphere. Nature 452:206–209

Nakamura H, Sampe T, Tanimoto Y, Shimpo A (2004) Observed associations among storm tracks, jet streams and midlatitude oceanic fronts. Geophys Monogr Ser

O'Reilly CH, Czaja A (2015) The response of the Pacific storm track and atmospheric circulation to Kuroshio Extension variability. Q J R Meteorol Soc 141:52–66

O'Reilly CH, Minobe S, Kuwano-Yoshida A (2016) The influence of the Gulf Stream on wintertime European blocking. Clim Dyn 47:1545–1567

Pawson S, Fiorino M (1999) A comparison of reanalyses in the tropical stratosphere. Part 3: inclusion of the pre-satellite data era. Clim Dyn 15:241–250

Pena-Ortiz C, Gallego D, Ribera P, Ordonez P, Alvarez-Castro MDC (2013) Observed trends in the global jet stream characteristics during the second half of the 20th century. J Geophys Res Atmos 118:2702–2713

Ronalds B, Barnes E, Hassanzadeh P (2018) A barotropic mechanism for the response of jet stream variability to arctic amplification and sea ice loss. J Clim 31:7069–7085

Schlesinger ME, Ramankutty N (1994) An oscillation in the global climate system of period 65–70 years. Nature 367:723–726

Sheldon L, Czaja A (2014) Seasonal and interannual variability of an index of deep atmospheric convection over western boundary currents. Q J R Meteorol Soc 140:22–30

Simpson IR, Yeager SG, McKinnon KA, Deser C (2019) Decadal predictability of late winter precipitation in western Europe through an ocean–jet stream connection. Nat Geosci 12:613–619

Small RJ, Tomas RA, Bryan FO (2014) Storm track response to ocean fronts in a global high-resolution climate model. Clim Dyn 43:805–828

Spensberger C, Spengler T (2020) Feature-based jet variability in the upper troposphere. J Clim 33:6849–6871

Strong C, Davis RE (2007) Winter jet stream trends over the Northern Hemisphere. Q J R Meteorol Soc 133:2109–2115

Sung M-K, An S-L, Kim B-M, Woo S-H (2014) A physical mechanism of the precipitation dipole in the western United States based on PDO-storm track relationship. Geophys Res Lett 41:4719–4726

Torrence C, Compo GP (1998) A practical guide to wavelet analysis. Bull Am Meteor Soc 79:61–78

Trenberth KE, Caron JM (2001) Estimates of meridional atmosphere and ocean heat transports. J Clim 14:3433–3443

Trenberth KE, Hurrell JW (1994) Decadal atmosphere-ocean variations in the Pacific. Clim Dyn 9:303–319

van der Swaluw E, Drijfhout SS, Hazeleger W (2007) Bjerknes compensation at high northern latitudes: the ocean forcing the atmosphere. J Clim 20:6023–6032

Wang XL, Feng Y, Compo GP, Swail VR, Zwiers FW, Allan RJ, Sardeshmukh PD (2013) Trends and low frequency variability of extra-tropical cyclone activity in the ensemble of twentieth century reanalysis. Clim Dyn 40:2775–2800

Whitaker JS, Compo GP, Wei X, Hamill TM (2004) Reanalysis without radiosondes using ensemble data assimilation. Mon Weather Rev 132:1190–1200

Woollings T, Hannachi A, Hoskins B (2010) Variability of the North Atlantic eddy-driven jet stream. Q J R Meteorol Soc 136:856–868

Woollings T, Czuchnicki C, Franzke C (2014) Twentieth century North Atlantic jet variability. Q J R Meteorol Soc 140:783–791

Woollings T, Franzke C, Hodson DLR, Dong B, Barnes EA, Raible CC, Pinto JG (2015) Contrasting interannual and multidecadal NAO variability. Clim Dyn 45:539–556